Electronic Supplementary Material (ESI) for Dalton Transactions.
This journal is © The Royal Society of Chemistry 2022

Construction of fast Li-ion path in MOF-derived Fe_3O_4@NC sulfur host enables high-rate lithium-sulfur battery

Yifang Zhao,[†a] Lian Wu, [†a] Yue Yu,[a] Yongqiang Dai,[a] Bing Liao,*[b] and Hao Pang*[a]

a. *Guangdong Provincial Key Laboratory of Industrial Surfactant, Institute of Chemical Engineering, Guangdong Academy of Sciences, Guangzhou, Guangdong 510665 (P. R. China).*

b. *Guangdong Academy of Sciences, Guangzhou, Guangdong 510070 (P. R. China).*

† *These authors contributed equally to this work.*

* *Corresponding authors. E-mail address: liaobing@gic.ac.cn; panghao@gdcri.com.*

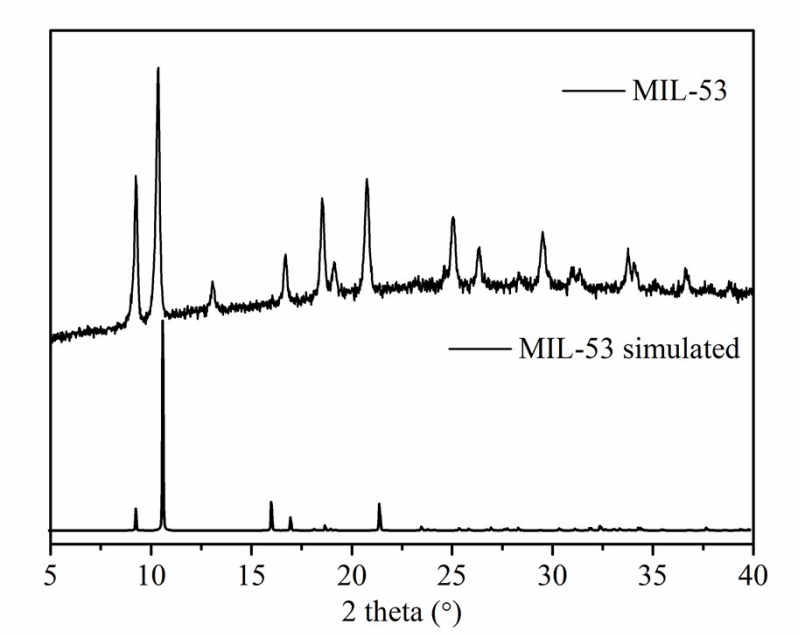

Figure S1. XRD patterns of the as-synthesized and simulated MIL-53 (Fe).

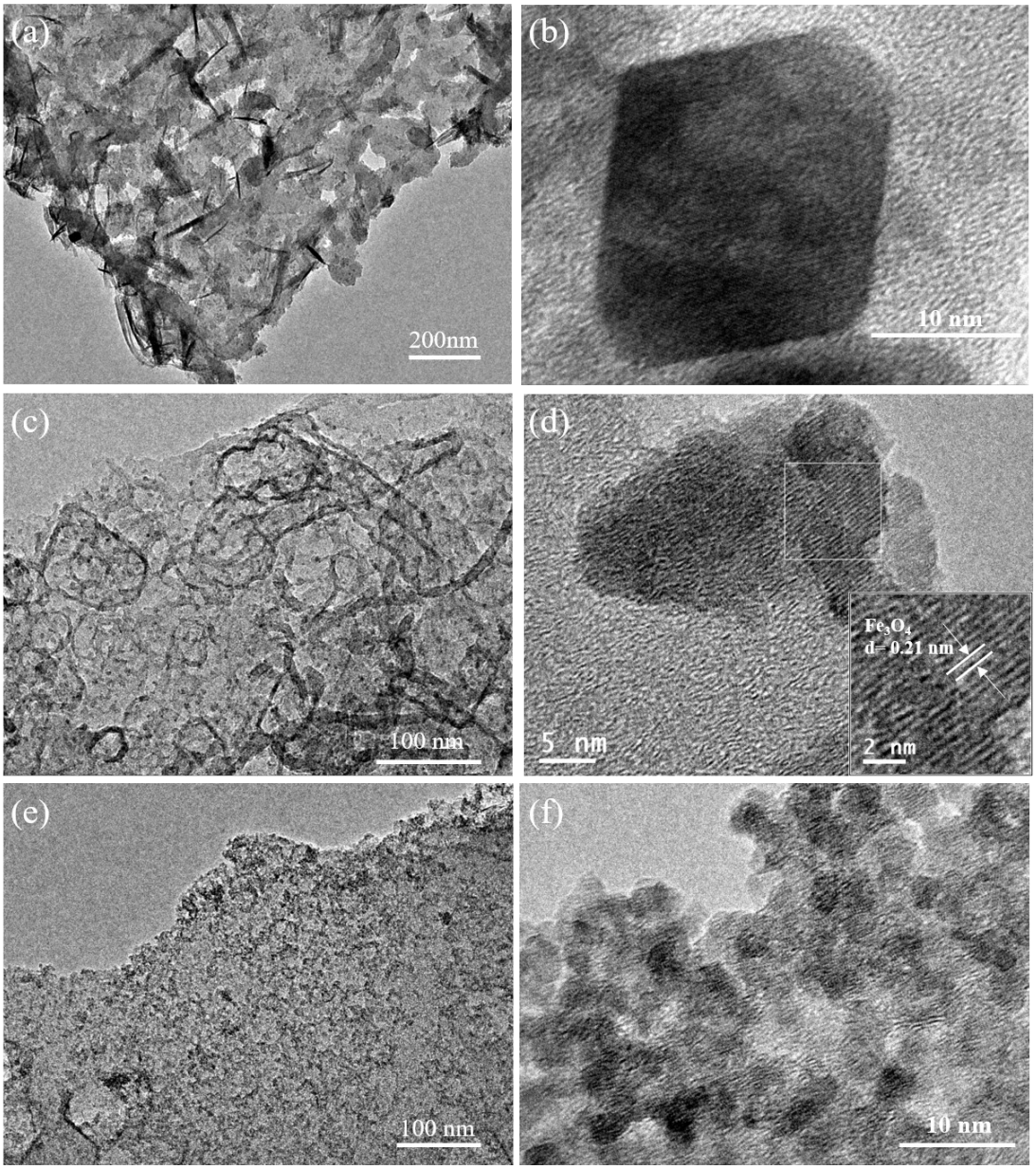

Figure S2. TEM images of LK450 (a, b), LK700 (c, d) and Li700 (e, f).

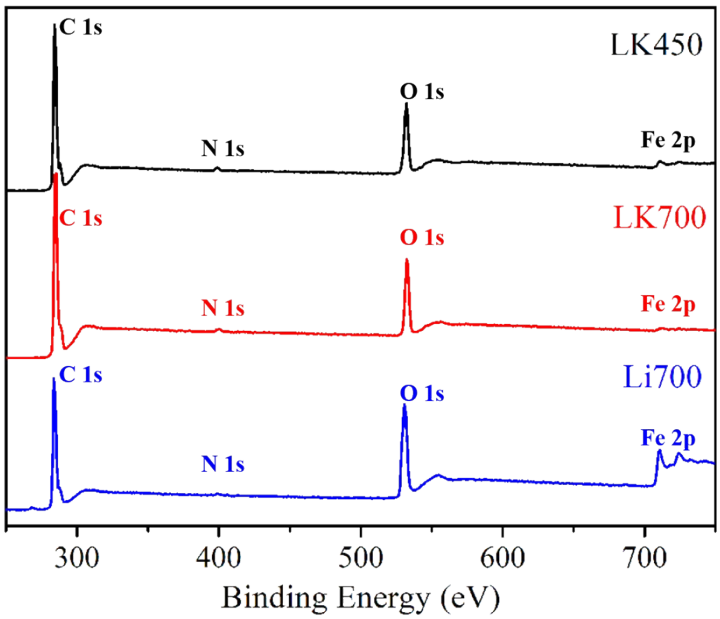

Figure S3. XPS survey spectra of LK450, LK700 and Li700.

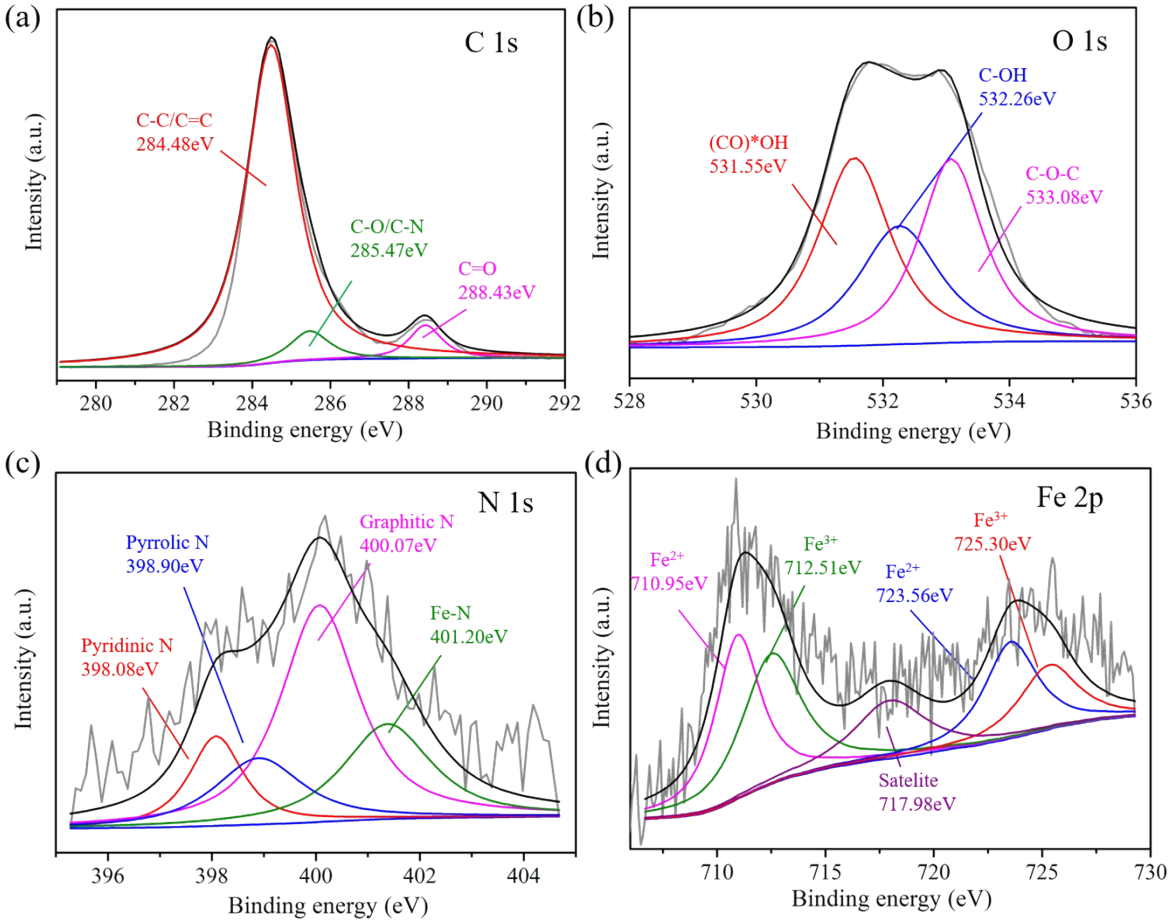

Figure S4. XPS spectrum of LK700. (a) C 1s, (b) O 1s, (c) N 1s and (d) Fe 2p XPS spectra of LK700.

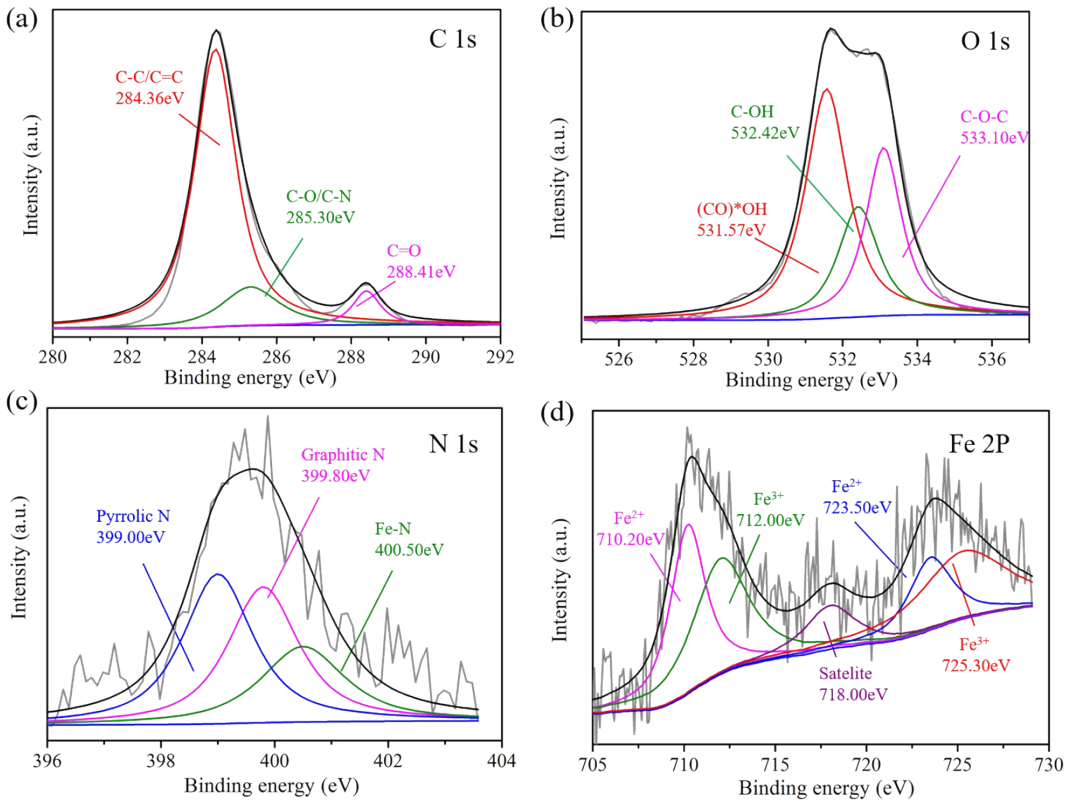

Figure S5. XPS spectrum of Li700. (a) C 1s, (b) O 1s, (c) N 1s and (d) Fe 2p XPS spectra of Li700.

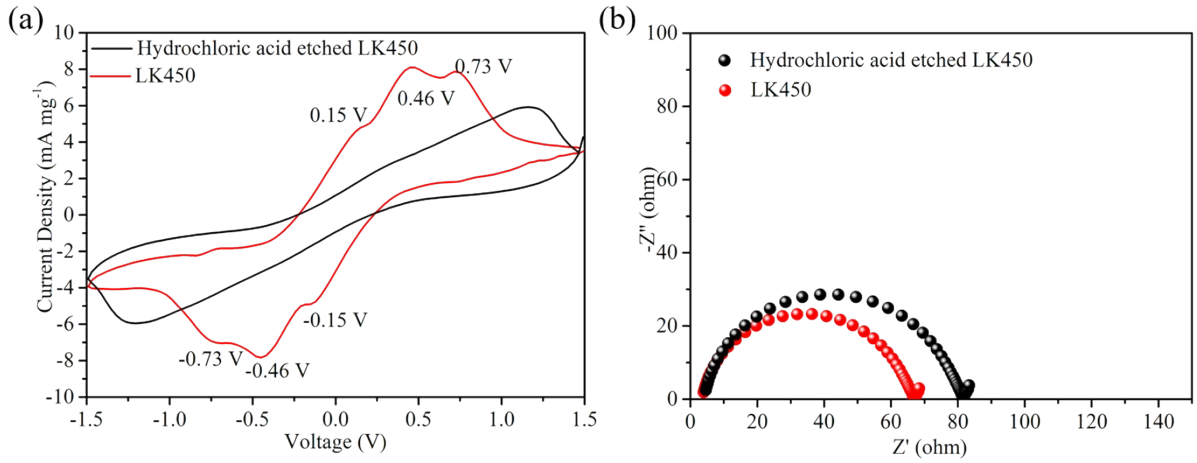

Figure S6. (a) CV curves and (b) EIS profiles of the symmetric Li_2S_6 cells with Fe_3O_4@NC and NC electrodes.

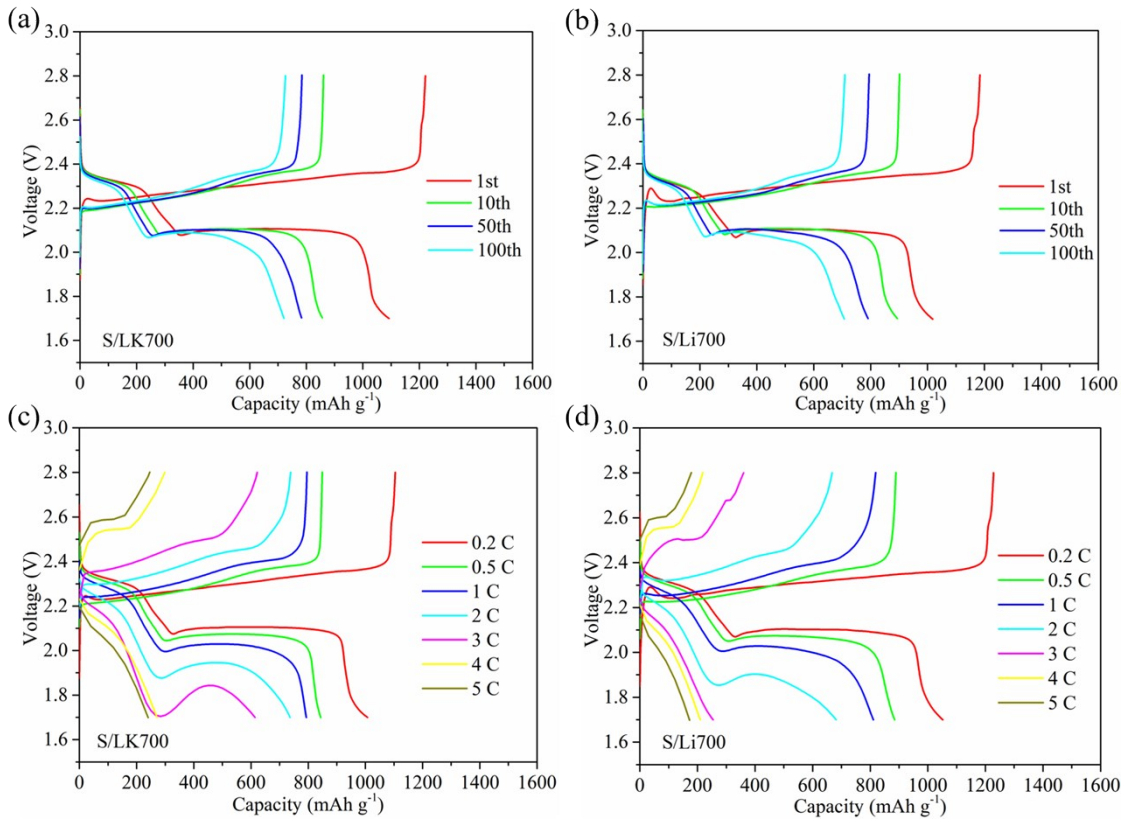

Figure S7. Galvanostatic charge/discharge profiles of LK700 and Li700 cathodes at various cycles (0.2 C) (a, b) and various C-rates (c, d).

Table S1. Contents of C, N, O, H, and Fe in LK450, LK700 and Li700

Sample	C (wt%)	N (wt%)	O(wt%)	H (wt%)	Fe (wt%)
LK450	37.03	6.58	19.10	1.91	35.38
LK700	38.03	3.59	16.22	1.10	41.06
Li700	32.82	1.73	22.59	0.99	41.87

Table S2. Porosities of LK450, LK700 and Li700

Sample	S_{BET} ($m^2 \cdot g^{-1}$)	Pore volume ($cm^3 \cdot g^{-1}$)
LK450	182.58	0.32
LK700	210.32	0.15
Li700	222.09	0.12

Table S3 Values of R_s, R_{ct} and W_C for various Li-S cells.

Cathode used in the Li-S cell	R_s (Ω)	R_{ct} (Ω)	*Wc* (Ω)
S/LK450	4.5	61.7	13.7
S/LK700	3.6	83.6	44.8
S/Li700	3.7	59.1	76.8

Table S4 Values of K_{C1}, K_{C2}, and K_A, and the corresponding D_{Li} of S/LK450, S/LK700 and S/Li700.

Cathode used in the Li-S cell	K_{C1}	D_{Li} ($cm^2 \cdot s^{-1}$)	K_{C2}	D_{Li} ($cm^2 \cdot s^{-1}$)	K_A	D_{Li} ($cm^2 \cdot s^{-1}$)
S/LK450	3.36	1.53×10^{-5}	5.53	4.14×10^{-5}	8.63	10.1×10^{-5}
S/LK700	3.27	1.45×10^{-5}	3.11	1.31×10^{-5}	7.91	8.46×10^{-5}
S/Li700	2.38	0.77×10^{-5}	3.45	1.61×10^{-5}	7.15	6.92×10^{-5}

Table S5. Performance comparison of S/Fe_3O_4@carbon cathode with other reported sulfur cathodes.

Materials	Sulfur content (wt%)	Sulfur loading ($mg \cdot cm^{-2}$)	Rate performance (C, mAh g^{-1})	Cycling performance				References
				Current Rate (C)	Cycles	Initial capacity (mAh g^{-1})	Capacity retention (mAh g^{-1})	
Fe_3O_4@carbon-graphene	/	3.85	3 C, 755	0.1 C	100	1200	1007	[1]
Fe_3O_4@C	70	1.5	5 C, 505	1 C	300	760	755	[2]
Fe_3O_4@NC	60	1.5	2 C, 654	0.1	140	1006	662	[3]
Fe_3O_4@C	67.4	2.3	3 C, 674	0.2 C	100	1241	967	[4]
Fe_3O_4@C	71	1.5	5 C, 550	0.5 C	200	791	611	[5]
York-shell C@Fe_3O_4	80	2.2	2 C, 773	0.1	200	1366	1165	[6]
Fe_3O_4@NC	54	4.7	4 C, 531	0.2	1000	~1114	780	[7]
Fe_3O_4@graphene	60	0.478	2 C, 589	1 C	500	802	659	[8]
Fe_3O_4 nanospheres	70	1.5	2 C, 450	0.2 C	100	867	680	[9]
Fe_3O_4@C	70	1	1 C, 640	1 C,	300	819	642	[10]
Fe_3O_4@C-G	75	2	3 C, 748	0.2 C	100	1425	1102	[11]
Fe_3O_4-PNCT	70	1.5	5 C, 685	1 C	1000	930	612	[12]
LK450	**70**	**1.2**	**5 C, 528**	**0.2**	**200**	**1194**	**743**	**Our work**
				1	**500**	**845**	**702**	
		2.4	***I***	**0.2**	**200**	**825**	**669**	
		4.0	***I***	**0.2**	**100**	**811**	**673**	

Notes: NC: N-doped carbon; G: graphene

References

[1] M. Ding, S. Huang, Y. Wang, J. Hu, M. E. Pam, S. Fan, Y. Shi, Q. Ge, H. Y. Yang*, *J. Mater. Chem. A*, 2019, **7**, 25078–25087.

[2] G. Liu, K. Feng, H. Cui, J. Li*, Y. Liu, M. Wang*, *Chem. Eng. J*., 2020, **381**, 122652.

[3] S. Deng, Q. Li, Y. Chen, C. Wang, H. Zhao, J. Xu*, J. Wu*, X. Yao, *Inorg. Chem. Front*., 2021, **8**, 1771-1778.

[4] M. Yuan, Y. Zhao*, Z. Sun*, Z. Bakenov, *J. Electroanal. Chem*., 2020, **877**, 114608.

[5] Y. Huang, Z. Li, T. Zhu, X. Gao*, X. Lv, M. Ling, Z. Wan, Y. Xia*, *ACS Appl. Energy Mater.*, 2021, **4**, 3921−3927.

[6] J. He, L. Luo, Y. Chen*, A. Manthiram*, *Adv. Mater*., 2017, **29**, 1702707.

[7] K. Lu, H. Zhang, S. Gao, H. Ma*, J. Chen, Y. Cheng*, *Adv. Funct. Mater*., 2019, **29**, 1807309.

[8] Y. Liu, X. Qin*, S. Zhang, G. Liang, F. Kang, G. Chen, B. Li*, *ACS Appl. Mater. Interfaces*, 2018, **10**, 26264−26273.

[9] N. Zhang, B. D. A. Levin, Y. Yang, D. A. Muller, H. D. Abruña*, *J. Electrochem. Soc*., 2018, **165**, 1656-1661.

[10] L. Fan, H. Wu, X. Wu, M. Wang, J. Cheng, N. Zhang*, Y. Feng*, K. Sun, Electrochimica Acta, 2019, **5**, 444-451.

[11] H. Li, J. Wang, Y. Zhang*, Y. Wang, A. Mentbayeva, Z. Bakenov, *J. Power Sources*, 2019, **437**, 226901.

[12] S. Xin, J. Li, H. Cui, Y. Liu, H. Wei, y. Zhong, M. Wang*, *Chem. Eng. J*., 2021, **410**, 128153.